CLM - P 155

United Kingdom Atomic Energy Authority

RESEARCH GROUP

Preprint

Classification of $3p^n - 3p^{n-1}$ 4s, 5s, 4d, 5d transitions in elements of the iron period and oscillator strengths in iron and nickel from atomic self-consistent field calculations.

B. C. FAWCETT
N. J. PEACOCK
R. D. COWAN

Culham Laboratory
Abingdon Berkshire

1968

UNCLASSIFIED
(Approved for Publication)

CLM - P 155

CLASSIFICATION OF $3p^n - 3p^{n-1}$ 4s,5s,4d,5d TRANSITIONS IN ELEMENTS OF IRON PERIOD AND OSCILLATOR STRENGTHS IN IRON AND NICKEL FROM ATOMIC SELF-CONSISTENT FIELD CALCULATIONS

By

B.C. FAWCETT
N.J. PEACOCK
R.D. COWAN*

(Submitted for publication in Proc. Phys. Soc.)

A B S T R A C T

Term values and oscillator strengths in highly ionized ions of the iron period are calculated via the Slater theory of atomic structure and are used to identify laboratory spectra of $3s^2\ 3p^n - 3s^2\ 3p^{n-1}$ 4s , 5s , 4d , 5d transitions in the argon, chlorine and sulphur isoelectronic sequences. New classifications are made in argon, scandium, titanium, vanadium, manganese and iron. The isoelectronic data and the theoretical calculations are used to identify lines in the solar spectrum between 50 and 110 Å. The calculated oscillator strengths of resonance transitions in Fe IX to Fe XIV and Ni XI to Ni XIV are tabulated.

* Los Alamos Scientific Laboratory, Los Alamos, New Mexico, USA.

U.K.A.E.A. Research Group,
Culham Laboratory,
Abingdon,
Berks.

January, 1968

1. INTRODUCTION

Observations of the complex emission line spectrum from the sun in the far vacuum ultraviolet e.g. Tousey et al.(1965), Manson (1967), have stimulated interest in the classification of multiplets of highly-ionized ions of the first long period in which iron and nickel are important solar elements. Methods of iso-electronic extrapolation have proved successful in the identification of highly ionized ions of these elements using the data from various laboratory plasma sources, e.g. Gabriel, Fawcett and Jordan (1965), Fawcett, Gabriel and Saunders (1967). This technique is often frustrated however by the changing relative multiplet intensities throughout the sequences due to changes in coupling, and by the gaps in the experimental data for any one configuration. However purely theoretical calculations of the term structure of high ionized ions based on the Slater theory of atomic structure can give good agreement with the measured term values and can lead to positive identifications of new multiplets when compared to laboratory spectra, e.g. Cowan and Peacock (1965), Cowan (1967(a)).

The present paper presents a further comparison between refined calculations (Cowan 1966; 1967,b) and the emission spectra from the plasma sources described. This leads to new identifications in ions isoelectronic with Fe X, XI, particularly those ions Ti VI, VII and Mn IX, X for which the multiplets of interest were intense and relatively well-resolved. The theoretical programme computes line strengths from the intermediate coupling wave functions which are a by-product of the energy level calculations and it has been thought worthwhile to list the theoretical values of the strongest transitions for the astrophysically important ion species such as Fe IX to Fe XIV and Ni XI to Ni XIV. The configurations $3p^n - 3p^{n-1}$ 4s, 4d in these ions should contribute significantly to the intensity of solar emission between 50 and 100 Å.

2. EXPERIMENTAL SPECTRA

Several diverse laboratory high-temperature sources were used to excite emission spectra from ions considered in this paper. A C-strap, theta-pinch was used for the lower ionization stages, e.g. Fe VIII, IX (Fawcett and Gabriel, 1965). A high voltage vacuum spark could be made to produce rather higher ionization stages, which were varied by changing the inductance in series with the spark gap and by operating the spark over a range of applied voltages from 30 kV to 100 kV. With this source classification of the recorded spectral lines into separate ionization stages was aided through the use of a microsecond shutter; this permitted the spectra to be recorded at different times during the spark when the emission from particular ions was most intense. In order to isolate the particular ions Fe XII, XIII, XIV, the large toroidal Z-pinch Zeta operated under high exciting conditions proved to be the most useful source (Gabriel, Fawcett and Jordan, 1965).

The emission from a plasma produced when a solid target is irradiated by a focussed, Q-spoiled Ruby laser beam was also studied but the dominant ionization stage was difficult to control (Burgess, Fawcett and Peacock, 1967). However, where there were wavelength coincidences in the spectrum of the pure laser-produced plasma and the spectrum from other sources e.g. Zeta, it was possible to differentiate between different elements emitting sinultaneously from Zeta.

The emission spectra were recorded photographically using a two-metre, grazing-incidence spectrograph of the type described by Gabriel, Swain and Waller (1965), with a 600 line/mm platinised replica grating and an entrance slit 3 to 5 microns wide. The slit assembly incorporated a mechanical shutter with a microsecond time resolution (Fawcett and Gabriel, 1966).

The lines of Argon identified in Table 1 were emitted from an electrodeless discharge and recorded with a 3-metre normal-incidence spectrograph.

The ionization stages of the unknown lines were identified by comparing their intensities under different conditions of excitation with the intensities of known multiplets of ions on the same micro-photometer plot.

3. COMPARISON OF HX CALCULATIONS WITH LABORATORY SPECTRA

Calculations of the energy levels involved were made with the aid of the Slater-Condon theory of atomic structure (Cowan 1966). The effects of configuration interaction were not included. The required values of E_{av} and of the electrostatic and spin-orbit parameters F_k, G_k and ζ_i for each configuration of interest (and of the dipole radial integral needed to compute absolute oscillator strengths) were calculated in the usual way from radial wave functions; these functions were computed using an approximation to the Hartreee-Fock equations which is equivalent to the Hartree theory plus a statistical allowance for exchange. This approximation is referred to as HX by Cowan (1967b). The computed parameter values were multiplied by correction factors (0.85 for all F_k, G_k and ζ_i, except 0.95 for $\zeta_{(3p)}$) known empirically to be required for good agreement with experiment. The modified values were then used as input to a computer programme (Cowan, 1966) which calculated all energy levels, wavelengths and oscillator strengths for each transition of interest.

Schematic computed spectra (such as those shown in Figs.1 and 2 for $3p^4 - 3p^3 4d$ and $3p^5 - 3p^4 4d$ transitions in Ti and Mn) were plotted, using as ordinate the calculated value of gf for each possible line satisfying the selection rule $\Delta J = 0, \pm 1$. (These ordinates represent theoretical relative intensities within a given transition array,

to the approximation that λ^3 is constant, all states of the upper configuration are equally excited, and self-absorption is negligible. Previous work (Cowan and Peacock, 1965) has shown that in the absence of configuration interaction the calculated wavelength for the centre of gravity of a multiplet in a high-ionization spectrum lies within about 2% of the observed wavelength; by itself, this is sufficiently close only to identify the transition array to which observed lines probably belong. However, calculated multiplet splittings are correct to within about 10% (0.1 Å in the wavelength region considered here), and this together with the predicted relative intensities is generally sufficient to yield detailed line identifications.

Since the $3p^n - 3p^{n-1}4s,5s,4d,5d$, etc. transitions in the ions Fe IX to Fe XIV should contribute to the solar spectrum between 40 Å and 110 Å the wavelengths and intensities of these lines were computed for iron. Iso-electronic ions of higher and lower ionization, including the neutral atoms were also computed.

Those line pairs are readily identified which have a wave number separation corresponding to an interval splitting in the ground configuration, which fortunately is documented for most of the ions considered here (Moore, 1949). In a semi-empirical fashion, confirmation was obtained firstly through checking the spin-orbit splitting between levels of the same term with different inner quantum number J using the regular doublet law. Secondly, the irregular doublet law was applied to the difference between the energy of the observed transition and the energy of the equivalent hydrogenic transition (Edlen 1964). In a few cases iso-electronic sequences could be linked with known lines of argon (Minnhagen 1963), however in most cases the irregular doublet law only checked the consistency through the sequences of the identified transitions.

4. NOTATION

In this paper we distinguish among like LS terms within a given configuration $3p^m\, n\ell$ by giving within parentheses the parent term of $3p^m$ which the theoretical calculations indicate to contribute most strongly to the term in question (Cowan and Peacock, 1965). In the case of $3p^m\, 3d$ this differs from the customary usage (Gabriel et al, 1966; Fawcett et al, 1967; Svensson and Eckberg, 1967) where the parent-term notation is chosen to be the lowest possible term of p^m for the lowest-energy LS term of $p^m\ell$, the next-to-lowest possible term of p^m for the next-to-lowest LS term of $p^m\ell$, etc. In order to indicate this type of energy ordering in $p^m\ell$, we shall in cases of ambiguity (principally in Fig.3 and Table 4) denote the energy ordering by primes; 3d for terms normally thought of as being based on the lowest parent, 3d′ for those thought of as being based on the next-to-lowest parent, 3d″ for the third lowest, etc. (c.f. Moore, 1949). For example, the highest ^2D in Ti VI 3d is normally denoted $3p^4(^1S)3d\ ^2D$, but will here be designated $3p^4(^3P)3d''\ ^2D$. That the highest-energy ^2D really is mostly $(^3P)^2D$ as computed, rather than $(^1S)^2D$ as usually written follows from the facts that the strongest $3p^5\ ^2P - 3p^4\ 3d\ ^2D$ lines arise from the highest-energy ^2D (borne out by the experimental observations, Cowan and Peacock, 1965), and from the selection rule that there is no change in parentage, the theoretical composition of $p^5\ ^2P$ being 60% $3p^4\ (^3P)$ and less than 7% $3p^4\ (^1S)$. The situation will be discussed further by Cowan in a later publication.

5. THE ARGON, CHLORINE AND SULPHUR ISO-ELECTRONIC SEQUENCES

Of the transitions considered in this paper only the $3p^n - 3p^{n-1}4s$ lines have been classified in the Argon, Chlorine and Sulphur sequences as far as Fe IX, X, XI (Kruger et al, 1937; Edlen, 1937 a,b), except that some $3p^n - 3p^{n-1}$ 4d, 5s lines in the Argon sequence have been classified by Alexander et al, (1965).

The present work extends the classification to include the $3p^{n-1}$ 4d,5d,5s configurations. The best experimental data were obtained using the vacuum spark source with elements of scandium, titantium and manganese, and the measure of agreement between experiment and calculation is best discussed for these elements. A microphotometer trace of the vacuum spark spectrum is shown for titanium in Fig.1 and for manganese in Fig.2. It is readily observed that the calculations give an excellent qualitative fit to the laboratory intensities for the transitions identified in the figures. The calculations predict relative line intensities rather well, not only within a given multiplet but also from one multiplet to another; furthermore the intensities of lines such as $3p^5\ ^2P - 3p^4(^3P)\ 4d\ ^4F$ and $3p^5\ ^2P - 3p^4(^3P)\ 4d\ ^2F$ in Ti VI (which appear to violate the LS-coupling selection rules) would be particularly difficult to assess without the help of the theoretical intermediate-coupling calculations. The procedure outlined in section 3 enables an analysis of the most intense unclassified lines belonging to the S I and Cℓ I isoelectronic sequences of titanium and in some cases of scandium, vanadium and manganese. These are listed in Table 1. The identifications in titanium agree precisely in almost every case with parallel work by Svensson and Ekberg (1967).

6. ARGON SPECTRA

In addition to the newly classified singlet lines of Argon III listed in Table 1, lines from transitions of the type $3p^4\ {}^3P - 3p^3 4d\ {}^3D$ from all three parents were observed at wavelengths in agreement with those already listed (Boyce 1935, Moore 1949). Emission lines due to transitions $3p^3 - 3p^2\ 4s$ in Argon IV were also observed. Listed values (de Bruin 1936, Moore 1949) of the $4s\ {}^4P$ and $4s\ {}^2P$ terms are correct; however, the $4s\ {}^2D$ term values are not in agreement with the following newly classified emission lines of A IV:

$3p^3\ {}^2D_{2\frac{1}{2}} - 3p^2({}^1D)\ 4s\ {}^2D_{2\frac{1}{2}}$	405·54 Å
$3p^3\ {}^2P_{1\frac{1}{2}} - \quad {}^2D_{2\frac{1}{2}}$	429·69 Å
$\frac{1}{2} \qquad\qquad 1\frac{1}{2}$	429·36 Å

7. THE IRON SPECTRUM - Fe X, XI

The only new lines of iron which have been positively identified (see Table 1) in the present spectra are $3p^5\ {}^2P_{\frac{1}{2},\frac{3}{2}} - 3p^4({}^3P)4d\ {}^2D_{\frac{3}{2},\frac{5}{2}}$ in Fe X. However, the observed data for titanium, vanadium, etc allow an extrapolation for addition lines through the iso-electronic sequence as far as iron, and these extrapolated values (E) are also listed with an estimated accuracy of ± 0.3 Å.

Confidence in the use of the theoretical calculations to check the semi-empirical extrapolation through to iron stems from the previous excellent agreement between experimental and calculated wavelengths in the case of the $3p^n - 3p^{n-1}\ 3d$ transitions of Fe VIII to Fe XVI (Cowan and Peacock 1965; Cowan 1967a; Gabriel, Fawcett and Jordan, 1965; Fawcett and Gabriel, 1966; Fawcett et al. 1967; Peacock et al. 1967). The variation in the difference between the calculated and experimental wave numbers for several of the strongest

previously identified transitions in Fe IX to Fe XIV are plotted in Fig.3. The modification factors (0·85 and 0·95) for the F, G and ζ parameters used in the theoretical calculations were chosen empirically for a best fit to the iron spectra and were assumed constant throughout the isoelectronic sequence. Differences between the calculated and the observed wave numbers lay on smoothly varying curves (Fig.3) showing no strong perturbation throughout the sequences. The deviation of the difference between theory and experiment from a smooth curve never exceeded 500 cm^{-1} in Fig.3 and was largest for some unexplained reason around titanium in the iso-electronic sequence. Mostly the deviation from the smooth difference curve was much less than 500 cm^{-1} and the curve could be used to predict the extrapolated wavelengths to 0·1 Å in the wavelength region studied here.

The effects of coupling changes and configuration interaction could affect the reliability of these iso-electronic extrapolations and consequently they are now discussed.

In Fig.3 the curves labelled g,h,j which lie well above the other transitions and thus show a large difference between the present theory and experiment are expected to be displaced because of configuration interaction. Garstang (1962) has discussed the interaction of the (j) term $3s^2 3d\ ^2D$ in Fe XIV with the term $3s\ 3p^2\ ^2D$; the whole multiplet $3p\ ^2p - 3d\ ^2D$ is thereby shifted uniformly to shorter wavelengths. In Fe X $3p^4\ (^1D)3d'\ ^2S_{1/2}$ interacts with $3s\ 3p^6\ ^2S_{1/2}$, and in Fe XI $3p^3\ (^2P)3d''\ ^1P$ and $(^2D)3d''\ ^3P$ levels are perturbed by the terms $3s2p^5\ ^1P, ^3P$, which causes the corresponding difference curves to lie off the graph in Fig.3. Presumably the large difference between calculation and experiment for the transitions (g) and (h) Fig.3 can be attributed to effects of analogous configuration interactions.

In contrast to the above examples of configuration interaction, observed $3p^n - 3p^{n-1}$ 4d, 4s transitions in the Cℓ I and S I iso-electronic sequences all agree well with the theoretically computed wavelengths. Plots analogous to Fig.1 are smooth curves lying close to $\sigma_{obs} - \sigma_{calc} = 0$. This means that configuration interaction effects are much smaller than for 3d (where strong perturbing levels are close) and the observed transitions in Ar to Mn can be extrapolated (with the calculation as a guide) to give the estimated Fe X, XI wavelengths shown in Table 1.

8. THE IRON SPECTRUM. Fe XII, XIII

The lack of data for ions iso-electronic with Fe XII and Fe XIII for the $3p^n - 3p^{n-1}$ 4d,4s transitions did not admit of the above extrapolation techniques. Moreover the best available spectra of these transitions (from Zeta) were weak in intensity and often blended, due to inadequate wavelength resolution together with the small multiplet splittings. A list of the wavelengths and intensities of the iron emission lines which appear in the relevant wavelength range from the Zeta source operated under the conditions when Fe XII and Fe XIII radiate most strongly, is shown in Table 2. The HX calculations of the term values should be accurate here to about ± 1 Å so that direct comparison of the calculation and the listed lines allows a tentative identification of the $3p^n - 3p^{n-1}$ 4d, 4s transitions. The range of the spectrum over which the strongest transitions of these configurations are calculated to occur is included for direct comparison with the measured wavelengths in Table 2.

In the laboratory and in the solar spectrum of these ions of iron, the transitions from the 4s levels to the ground level are more

intense than those originating from the 4d levels. The calculated gf values (Table 4) would indicate the reverse situation. The explanation may involve the collisional exchange rates within the levels of the $n = 4$ shell, and the relevant f-values can be estimated from the wavelengths of the transitions arising from the 4s,4p,4d,4f levels in Table 2.

9. APPLICATION TO THE SOLAR SPECTRUM FROM 50 Å TO 110 Å

Wavelengths of the line spectrum from the quiet sun between 30 Å and 128 Å have been measured to 0·1 Å or better by Manson (1967). Some identifications are included in Manson's paper. Other identifications have been made previously by Tousey et al. (1965).

The solar line identifications at wavelengths shorter than 110 Å are now reassessed taking into account two factors previously neglected. Firstly the relatively high intensity of those lines which can be excited directly from the ground level (Gabriel, Fawcett and Jordan, 1965) is considered. Secondly the high intensity of the $3p^n - 3p^{n-1}$ 3d transitions in Fe VIII to Fe XIV in the sun would seem to indicate that the transitions $3p^n - 3p^{n-1}$ 4d,4s discussed above should also contribute to the solar emission at wavelengths shorter than 110 Å. The identifications have been taken from the present work (*) and from the list of Vacuum Ultra-Violet Emission Lines by Kelly (1959) and are shown in Table 3. The present analysis includes only the more reliable identifications which result from transitions directly to the ground level. Due to the limited wavelength resolution in the solar spectrum and in the present laboratory iron spectrum and the probability of blended lines in both, some of the identifications are marked tentative ( ), Table 3.

10. OSCILLATOR STRENGTHS IN Fe and Ni

An analysis of the spectral line intensities in terms of the excitation conditions in the sun (Jordan 1966, Pottasch 1967) requires a knowledge of the oscillator strengths. The HX calculations of the iron and nickel oscillator strengths are listed for this purpose in Table 4 and cover the $3p^n - 3p^{n-1}$ 3d, 4d,4s configurations in Fe IX through to Fe XIV. The general agreement between the intensities of the laboratory spectra and the HX calculations lends confidence to the f-values, particularly where effects of configuration interaction can be neglected. The agreement where the data overlap with Hartree-Fock calculations of C. Froese (Pottasch 1967) is quite close and is within the difference (typically 10% for the $3p^{n-1}$ 3d levels) between the present values and those calculated using the method of Bates and Damgaard (1949).

11. CONCLUSIONS

The strongest lines arising from the configurations $3p^{n-1}$ 4d,4s,5d,5s in Ti VI and VII and in the iso-electronic ions of manganese have been identified with the aid of theoretical calculations. The observed relative line intensities, including intercombination lines are predicted to a good accuracy by the computations. This and the calculated term values lead to positive identification of multiplets which would be difficult by semi-empirical methods. Iso-electronic extrapolation through to iron, with the added confidence provided by the computations through the sequence, leads to predicted wavelengths of these configurations in Fe X and Fe XI.

Despite the poor experimental intensities of Fe XII, Fe XIII, comparison with the theory allows a separation of the ion stages in

the observed spectra and a tentative identification of the configurations responsible for the observed lines from these ions.

The agreement between ab initio theory and experiment leads us to tabulate the f-values for the strongest transitions in Fe IX to Fe XIV and Ni XI to Ni XIV which will be necessary in any analysis of the solar vacuum far ultra-violet spectrum.

REFERENCES

Alexander, E., Feldman, U., Fraenkel, B.S., 1965, Journ. Opt. Soc. America, 55, pp.650-653.

Bates, D.R. and Damgaard, A., 1949, Phil. Trans. Roy. Soc. London, A242, 101.

Beckman, A., 1937, Bidrag till Kannedomen om Skandiums Spektrum i Yttersta Ultraviolett (Uppsala: Almquist och Wiksells).

Boyce, J.C., 1935, Phys. Rev., 48, pp.396-402.

Burgess, D.D., Fawcett, B.C. and Peacock, N.J., Proc. Phys. Soc., 1967.

Cowan, R.D. and Peacock, N.J., 1965, Astrophys. J., 142, pp.390-6, erratum, ibid 143, 283, (1966).

Cowan, R.D., 1966, Jnl. Opt. Soc. Am., 56, 1416; further details to be published.

Cowan, R.D., 1967 (a), Astrophys. J., 147, pp.377-379

Cowan, R.D., 1967 (b), Phys. Rev., 163, pp.54-61.

de Bruin, T.L., 1936, Physica, 3, No.8, pp.810-813.

Edlén, B., 1937, (a) Zeit. Phys., 104, pp.188-193.

Edlén, B., 1937, (b) Zeit. Phys., 104, pp.407-416.

Edlén, B., 1964, Handb. d. Phys., 27 (Berlin: Springer Verlag) pp.80-201.

Fawcett, B.C., Gabriel, A.H., 1965, Astrophys. J., 141, pp.343-353.

Fawcett, B.C., Gabriel, A.H. 1966, Proc. Phys. Soc., 88, pp.262-264.

Fawcett, B.C., Gabriel, A.H. and Saunders, P.A.H., 1967, Proc. Phys. Soc., 90, pp.863-867.

Gabriel, A.H., Swain, J.R. and Waller, W.A., 1965, J. Sci. Instr., 42, pp.94-97.

Gabriel, A.H., Fawcett, B.C. and Jordan, C., 1965, Nature, Lond., 206, pp.390-2.

Gabriel, A.H., Fawcett, B.C. and Jordan, C., 1966, Proc. Phys. Soc. 87, pp.825-39.

Garstang, R.H. ann. d'Astrophys (1962), 25, 109.

Jordan, C., 1966., Mon Not. Roy. Ast. Soc., 132, 463.

Kelly, R., 1959, Table of ultra-violet emission lines., UCRL 5612.

Kruger, P.G. and Pattin, H.S., 1937, Phys. Rev., 52, pp.621-625.

Kruger, P.G., Weissberg, S.G. and Phillips, L.W., 1937, Phys. Rev., 51, pp.1090-1091.

Manson, E., 1967, Astrophys. J., 147, pp.703-710.

Minnhagen, L., 1963, Ark. für Fysik, 25, no.19, pp.203-284.

Moore, C.E., 1949, Atomic Energy Levels, Nat. Bur. Standards, Circ. 467, (Washington: US Govt. printing office).

Peacock, N.J., Cowan, R.D. and Sawyer, G.A., 1967, Proc. 7th Int. Conf. on Ionization Phenomena in Gases, Belgrade, 1965 (Belgrade: Gradevinska Knjiga).

Pottasch, S.R., 1967, Bul. Ast. Inst. Netherlands., 19, 2, 113.

Svensson, L.A. and Ekberg, J.O., (Submitted to Ark. für Fysik) 1967.

Tousey, R., Austin, W.E., Purcell, J.D. and Wilding K.G., 1965, Ann. d'Astrophys., 28, pp.755-8.

TABLE 1

Wavelengths of Argon, Chlorine and Sulphur Isoelectronic Sequences

Classifications Based on Comparison of (HX) Calculations with Observed Spectra

(Figures in [ ] denote relative intensity)

Argon I Sequence $3p^6 - 3p^5$ nd, ns.						
TRANSITION	J	Sc IV	Ti V	V VI		
$3p^6\ ^1S - 3p^5(^2P_{\frac{1}{2}})\ 5d\ [\frac{3}{2}]$	0 - 1			117.7 [6]		
$3p^6\ ^1S - 3p^5(^2P_{\frac{3}{2}})\ 5d\ [\frac{3}{2}]$	0 - 1			118.7 [7]		
$3p^6\ ^1S - 3p^5(^2P_{\frac{3}{2}})\ 5d\ [\frac{1}{2}]$	0 - 1			119.3 [6]		
$3p^6\ ^1S - 3p^5(^2P_{\frac{1}{2}})\ 6s\ [\frac{1}{2}]$	0 - 1	174.57 [4]				
$3p^6\ ^1S - 3p^5(^2P_{\frac{3}{2}})\ 6s\ [\frac{3}{2}]$	0 - 1	175.89 [4]	146.87 [4]			
Chlorine I Sequence $3p^5 - 3p^4$ 4d, 5d, 5s.						
TRANSITION	J	Sc V	Ti VI	V VII	Mn IX	Fe X
$3p^5\ ^2P - 3p^4(^3P)\ 4d\ ^2D$	1.5 - 2.5		153.53 [8]	125.98 [8]	90.08 [9]	77.83 [8]
	1.5 - 1.5		153.36 [5]	125.87E	89.99 [8]	77.78E
	0.5 - 1.5		154.76 [5]	127.11B [4]	91.0 [8]	78.68 [4]
$3p^5\ ^2P - 3p^4(^3P)\ 4d\ ^2P$	0.5 - 1.5		153.25 [4]			
$3p^5\ ^2P - 3p^4(^3P)\ 4d\ ^4F$	1.5 - 2.5		152.94 [6]	125.62E	89.89 [4]	77.72E
$3p^5\ ^2P - 3p^4(^3P)\ 4d\ ^2F$	1.5 - 2.5		152.16 [6]	125.19E	89.77 [4]	77.67E
$3p^5\ ^2P - 3p^4(^1D)\ 4d\ ^2D$	1.5 - 2.5		148.29 [6]	121.93 [6]	87.52 [8]	75.76E
	1.5 - 1.5		148.00 [2]	121.80E	87.24 [3]	75.47E
	0.5 - 1.5		149.39 [6]	122.95B [4]	88.23 [5]	76.37E
$3p^5\ ^2P - 3p^4(^1D)\ 4d\ ^2P$	1.5 - 1.5		149.00 [7]	122.56 [5]	87.94 [6]	76.11E
	0.5 - 1.5		150.30 [4]	123.72E	88.89 [4]	77.03E
	0.5 - 0.5				88.74 [4]	
	1.5 - 0.5				87.79 [2]	
$3p^5\ ^2P - 3p^4(^1P)\ 4d\ ^2S$	1.5 - 0.5		149.56 [6]	123.13E	88.40 [6]	76.53E
	0.5 - 0.5		150.88E	124.30E	89.39E	77.45E

TABLE 1 (Continued)

TRANSITION	J	Sc V	Ti VI	V VII	Mn IX	Fe X
$3p^5\ ^2P - 3p^4(^1S)\ 4d\ ^2D$	1.5 - 2.5		141.96 [3]	117.2 [3]		
$3p^5\ ^2P - 3p^4(^3P)\ 5d\ ^2D$	1.5 - 2.5		129.71 [6]			
	1.5 - 1.5		129.40 [3]			
	0.5 - 1.5		130.39 [5]			
$3p^5\ ^2P - 3p^4(^3P)\ 5d\ ^4F$	1.5 - 2.5		128.44 [1]			
$3p^5\ ^2P - 3p^4(^1D)\ 5s\ ^2D$	1.5 - 2.5	180.14 [7]	136.71 [4]	108.3 E	73.8 E	62.8 E
	1.5 - 1.5	179.42 [3]	(136.67) [1]			
	0.5 - 1.5	180.82 [4]	(137.80) [2]			
$3p^5\ ^2P - 3p^4(^3P)\ 5s\ ^2P$	1.5 - 1.5	180.96 [4]	140.43 [6]			
	1.5 - 0.5	181.55 [1]	139.91 [3]			
	0.5 - 0.5		141.04B [5]			
$3p^5\ ^2P - 3p^4(^3P)\ 5s\ ^4P$	1.5 - 1.5		141.08B [5]			

Sulphur I Sequence

$3p^4 - 3p^3\ 4d, 5s.$

TRANSITION	J	A III	Sc VI	TiVII	Mn X	Fe XI
$3p^4\ ^3P - 3p^3(^4S)\ 4d\ ^3D$	2 - 3	396.37Y [8]	169.26 [7]	137.66 [6]	83.48 [7]	72.7 E
	1 - 2	398.17Y [5]	170.25 [5]	138.53 [4]	84.28 [4]	73.2 E
	0 - 1	398.91Y [2]	170.54 [3]	138.79 [2]	84.2 E	73.3 E
$3p^4\ ^1D - 3p^3(^2D)\ 4d\ ^1F$	2 - 3	382.61 [5]	166.35 [7]	135.79 [6]	82.78 [8]	72.1 E
$3p^4\ ^1D - 3p^3(^2D)\ 4d\ ^1D$	2 - 2	387.45 [4]	167.17 [4]	136.25 [3]	83.03 [4]	72.3 E
$3p^4\ ^1S - 3p^3(^2D)\ 4d\ ^1P$	0 - 1	389.49 [1]		136.79 [4]		
$3p^4\ ^1D - 3p^3(^2D)\ 5s\ ^1D$	2 - 2		152.60 [5]			
$3p^4\ ^3P - 3p^3(^4S)\ 5s\ ^3S$	2 - 1		154.29 [5]			
	1 - 1		155.10 [3]			
	0 - 1		155.36 [1]			
$3p^4\ ^1S - 3p^3(^2P)\ 5s\ ^1P$	0 - 1		154.52 [1]			
$3p^4\ ^1D - 3p^3(^2P)\ 5s\ ^1P$	2 - 1		147.90 [2]			
$3p^4\ ^3P - 3p^3(^2D)\ 5s\ ^3D$	2 - 3		(148.18) [3]			

Wavelengths in Å = accuracy ± 0.03 Å. B indicates blend.
Y = observed (Boyce 1935). E = extrapolated values, accuracy ± 0.3Å.

TABLE 2

Emission Lines in Zeta identified as Fe XII or Fe XIII (accuracy of wavelengths ± 0.05 Å)

WAVELENGTH, Å	INTENSITY	WAVELENGTH	INTENSITY	WAVELENGTH	INTENSITY
82.82	8	76.11	9	65.98	3
80.55 Blend	8	74.82	4	65.63	2
80.23	6	71.87	4	63.56	3
80.05	6	71.33	5	63.20	6
79.50	5	70.01	3	62.94	5
78.46	4	69.60	5	62.69	5
77.58	3	67.78	1	62.36	3
77.00	4	67.21	3	62.09	3
76.47	7	66.27	2		

Wavelength Range of Emission Lines due to $3p^m - 3p^{m-1}$ 4s,4d in Fe XII and Fe XIII.

Ion	Transition Array	Wavelength Range of Strongest Transitions Calculated by Hartree X Method Å
Fe XII	$3p^3 - 3p^2 4s$	78 - 85
Fe XII	$3p^3 - 3p^2 4d$	65 - 69
Fe XIII	$3p^2 - 3p4s$	74 - 79
Fe XIII	$3p^2 - 3p4d$	61 - 65

TABLE 2 (Continued)

Wavelength Range of Emission Lines due to

$3s^2\ 3p^{n-1}\ m\ell - 3s^2\ 3p^{n-1}\ m\ell'$ in FeXIV, XIII, XII, XI, X, IX.

Ion	Transition Array	Wavelength Range Calculated by Hartree X Method. Å
Fe XIV	4s - 4p	822 - 855
	3d - 4f	75 - 76
	3d - 4p	91 - 92
Fe XIII	3p 4s - 3p 4p	700 - 1082
	3p 3d - 3p 4f	78 - 85
	3p 3d - 3p 4p	98 - 107
Fe XII	$3p^2$ 4s - $3p^2$ 4p	800 - 1000
	$3p^2$ 3d - $3p^2$ 4f	84 - 90
	$3p^2$ 3d - $3p^2$ 4p	108 - 117
Fe XI	$3p^3$ 4s - $3p^3$ 4p	900 - 1000
	$3p^3$ 3d - $3p^3$ 4f	91 - 94
	$3p^3$ 3d - $3p^3$ 4p	121 - 125
Fe X	$3p^4$ 4s - $3p^4$ 4p	900 - 1100
	$3p^4$ 3d - $3p^4$ 4f	100 - 105
	$3p^4$ 3d - $3p^4$ 4p	137 - 145
Fe IX	$3p^5$ 4s - $3p^5$ 4p	900 - 1200
	$3p^5$ 3d - $3p^5$ 4f	112 - 118
	$3p^5$ 3d - $3p^5$ 4p	160 - 170

TABLE 3

The Solar Spectrum from 50 Å to 110 Å

Observed Wavelength ± 0.1 Å (Manson, 1967)	Ion	Transition	J
50.26	FeXVI	$3s^2S - 4p^2P$	$\frac{1}{2} - 1\frac{1}{2}$
50.61	SiX	$3p^2P - 3d^2D$	$\frac{1}{2} - 1\frac{1}{2}$
	FeXVI	$3s^2S - 4p^2P$	$\frac{1}{2} - \frac{1}{2}$
55.28	SiIX	$2p^3P - 3d^3P$	0 - 1
	SiIX	$2p^3P - 3d^3D$	0 - 1
61.06	SiVIII	$2p^4S - 3d^4P$	$1\frac{1}{2} - \frac{1}{2}, 1\frac{1}{2}, 2\frac{1}{2}$
61.60	SVIII	$2p^2P - 3s^2D$	$1\frac{1}{2} - 2\frac{1}{2}$
	SiIX	$2p^3P - 3s^3P$	0 - 1
62.80	MgIX	$2s^1S - 3p^1P$	0 - 1
63.22	SVIII	$2p^2P - 3s^2P$	$1\frac{1}{2} - 1\frac{1}{2}$
	(FeXIII	3p - 4d)	
67.26	(FeXII	3p - 4d)	
69.8	SiVIII	$2p^4S - 3s^4P$	$1\frac{1}{2} - \frac{1}{2}, 1\frac{1}{2}, 2\frac{1}{2}$
72.00 *	(FeXI	3p - 4d)	
72.32 *	(FeXI	3p - 4d)	
75.02	MgVIII	$2p^2P - 3d^3D$	
76.11	(FeXIII	$3p^3P - 4s^3P$)	0 - 1
77.77 *	FeX	$3p^2P - 4d^2D$	$1\frac{1}{2} - 2\frac{1}{2}$
78.38 *	(FeXII	3p - 4s)	
79.56 *	(FeXII	3p - 4s)	
79.98 *	(FeXII	3p - 4s)	
80.18 *	(FeXII	3p - 4s)	
80.55 *	(FeXII	3p - 4s)	
81.63	SiVII	$2p^3P - 3s^3D$	2 - 3

TABLE 3 (Continued)

Observed Wavelength ± 0.1 Å (Manson, 1967)	Ion	Transition	J
82.50 *	(FeIX	$3p^1S - 4d\ [\frac{3}{2}]$	0 - 1)
82.78	MgVIII	$2p^2P - 3s^2S$	
86.85	FeXI	$3p^3P - 4s^3D$	2 - 1,2,3
88.12	NeVIII	$2s^2S - 3p^2P$	$\frac{1}{2} - \frac{1}{2}.1\frac{1}{2}$
89.0	FeXI	$3p^3P - 4s^3S$	2 - 1
93.98	FeX	$3p^2P - 4s^2D$	$1\frac{1}{2} - 1\frac{1}{2}.2\frac{1}{2}$
95.38	FeX	$3p^2P - 4s^2P$	$1\frac{1}{2} - \frac{1}{2}$
	(MgVII	$2p^3P - 3s^3P$	0 - 1)
96.07	FeX	$3p^2P - 4s^2P$	$1\frac{1}{2} - 1\frac{1}{2}$
103.58	FeIX	$3p^1S - 4s\ [\frac{1}{2}]$	0 - 1
105.20	FeIX	$3p^1S - 4s\ [\frac{1}{2}]$	0 - 1

Values in brackets are tentative. Indentifications * are from the present study, Table 2.

TABLE 4

Weighted Oscillator Strengths gf based on modified Hartree-Fock-Slater (HX) Calculations
(Values of Σgf are for the entire transition array indicated.)

TRANSITION	J	ION	Observed Wave-length, λ,Å	gf	Σgf	ION	λ, Å	gf
$3p^6\ {}^1S - 3p^5 3d\ {}^1P_1$	0 - 1	FeIX	171.06	3.72	3.73	NiXI	148.37	3.25
$3p^6\ {}^1S - 3p^5({}^2P_{3/2})4d\ [3/2]$	0 - 1	FeIX	83.45	0.469	0.724	NiXI	63.3H	0.66
$3p^6\ {}^1S - 3p^5({}^2P_{1/2})4d\ [3/2]$	0 - 1	FeIX	82.44	0.241		NiXI	62.4H	0.32
$3p^6\ {}^1S - 3p^5({}^2P_{3/2})4s\ [3/2]$	0 - 1	FeIX	105.24	0.148	0.377	NiXI	78.64	0.165
$3p^6\ {}^1S - 3p^5({}^2P_{1/2})4s\ [1/2]$	0 - 1	FeIX	103.58	0.229		NiXI	77.28	0.20
$3p^5\ {}^2P - 3p^4({}^3P)3d''\ {}^2D$	3/2 - 5/2	FeX	174.58	6.51	16.8	NiXII	152.14	5.69
	1/2 - 3/2	FeX	175.26	4.02		NiXII	152.95	3.56
	3/2 - 3/2	FeX	170.58	0.268				
$3p^5\ {}^2P - 3p^4({}^3P)3d'\ {}^2P$	3/2 - 3/2	FeX	177.24	3.21		NiXII	154.15	2.86
	1/2 - 3/2	FeX	182.31	0.129				
	3/2 - 1/2	FeX	175.48	0.501				
	1/2 - 1/2	FeX	180.45	1.15				
$3p^5\ {}^2P - 3p^4({}^1D)3d\ {}^2S$	3/2 - 1/2	FeX	184.53	0.692				
	1/2 - 1/2	FeX	190.02	0.260				
$3p^5\ {}^2P - 3p^4({}^3P)4d\ {}^2D$	3/2 - 5/2	FeX	77.83	0.856	4.59			
	1/2 - 3/2	FeX	78.68	0.151				
$3p^5\ {}^2P - 3p^4({}^1D)4d\ {}^2D$	3/2 - 5/2	FeX	75.8 E	0.410				
	1/2 - 3/2	FeX	76.4 E	0.469				
$3p^5\ {}^2P - 3p^4({}^1D)4d\ {}^2P$	3/2 - 3/2	FeX	76.1 E	0.451				
$3p^5\ {}^2P - 3p^4({}^1D)4s\ {}^2D$	3/2 - 5/2	FeX	94.07	0.374	1.91			
	1/2 - 3/2	FeX	95.37	0.290				
$3p^5\ {}^2P - 3p^4({}^3P)4s\ {}^2P$	3/2 - 3/2	FeX	96.12	0.473				
	1/2 - 3/2	FeX	97.59	0.041				
	1/2 - 1/2	FeX	96.97	0.211				
	3/2 - 1/2	FeX	95.34	0.161				
$3p^5\ {}^2P - 3p^4({}^3P)4s\ {}^4P$	3/2 - 5/2	FeX	97.83	0.014				
	3/2 - 3/2	FeX	97.12	0.201				

TABLE 4 (Continued)

TRANSITION	J	ION	Observed Wavelength, λ, Å	gf	Σ gf	ION	λ, Å	gf
$3p^4\ ^3P - 3p^3(^4S)3d''\ ^3D$	2 - 3	FeXI	180.42	5.77	30.3	NiXIII	157.75	5.04
	1 - 2	FeXI	182.17	2.77				
	0 - 1	FeXI	181.13	1.39				
	2 - 2	FeXI	178.04	0.987				
$3p^4\ ^1D - 3p^3(^2D)3d''\ ^1F$	2 - 3	FeXI	179.75	6.55		Ni XII	157.56	5.74
$3p^4\ ^1D - 3p^3(^2D)3d''\ ^1D$	2 - 2	FeXI	184.78	2.69				
$3p^4\ ^3P - 3p^3(^2D)3d''\ ^3P$	2 - 3	FeXI	188.29	0.752				
	1 - 2	FeXI	192.87	0.161				
$3p^4\ ^3P - 3p^3(^4S)4d\ ^3D$	2 - 3	FeXI	72.7 E	0.905				
	1 - 2	FeXI	72.2 E	0.315	11.2			
$3p^4\ ^1D - 3p^3(^2D)4d\ ^1F$	2 - 3	FeXI	72.1 E	1.62				
$3p^4\ ^1D - 3p^3(^2D)4d\ ^1D$	2 - 2	FeXI	72.3 E	0.623				
$3p^4\ ^3P - 3p^3(^2D)4s\ ^3D$	2 - 3	FeXI	86.77	0.434				
	1 - 2	FeXI	87.99	0.134	3.86			
	0 - 1	FeXI	88.17	0.059				
	2 - 2	FeXI	87.03	0.203				
$3p^4\ ^3P - 3p^3(^4S)4s\ ^3S$	2 - 1	FeXI	89.19	0.459				
$3p^4\ ^1D - 3p^3(^2D)4s\ ^1D$	2 - 2	FeXI	89.10	0.786				
$3p^3\ ^2D - 3p^2(^3P)3d'\ ^2F$	5/2 - 7/2	FeXII	186.87	5.68	27.1	NiXIV	164.13	5.00
$3p^3\ ^4S - 3p^2(^3P)3d\ ^4P$	3/2 - 5/2	FeXII	195.14	2.37				
	3/2 - 3/2	FeXII	193.53	1.67				
	3/2 - 1/2	FeXII	192.42	0.875				
$3p^3\ ^2D - 3p^2(^1D)4d\ ^2F$	5/2 - 7/2	FeXII	66.2 H	0.907	13.1			
$3p^3\ ^4S - 3p^2(^3P)4d\ ^4P$	3/2 - 5/2	FeXII	66.1 H	0.524				
$3p^3\ ^2D - 3p^2(^1D)4s\ ^2D$	5/2 - 5/2	FeXII	80.3 H	0.505	3.85			
$3p^3\ ^4S - 3p^2(^3P)4s\ ^4P$	3/2 - 5/2	FeXII	79.5 H	0.381				

TABLE 4 (Continued)

TRANSITION	J	ION	Observed Wave-length, λ, Å	gf	Σgf	ION	λ, Å	gf
$3p^2\ ^3P - 3p3d\ ^3D$	2 - 3	FeXIII	203.80	2.34	12.1			
$3p^2\ ^1D - 3p3d\ ^1F$	2 - 3	FeXIII	196.65	3.35				
$3p^2\ ^3P - 3p4d\ ^3D$	2 - 3	FeXIII	62.1 H	0.649	7.53			
$3p^2\ ^1D - 3p4d\ ^1F$	2 - 3	FeXIII	62.9 H	1.78				
$3p^2\ ^3P - 3p4s\ ^3P$	2 - 2	FeXIII	74.8 H	0.442	1.95			
$3p^2\ ^1D - 3p4s\ ^1P$	2 - 1	FeXIII	76.0 H	0.561				
$3p\ ^2P - 3d\ ^2D$	3/2 - 5/2	FeXIV	219.11	1.26	2.13			
	1/2 - 3/2	FeXIV	211.34	0.728				
$3p\ ^2P - 4d\ ^2D$	3/2 - 5/2	FeXIV	59.58	0.983	1.64			
	1/2 - 3/2	FeXIV	58.96	0.552				
$3p\ ^2P - 4s\ ^2S$	3/2 - 1/2	FeXIV	70.8 H	0.247	0.372			
	1/2 - 1/2	FeXIV	69.9 H	0.125				

All wavelengths are observed values except those marked:

E = estimated wavelengths ± 0.3 Å based on isoelectronic extrapolation.

H = calculated wavelengths ± 1 Å based on HX calculations.

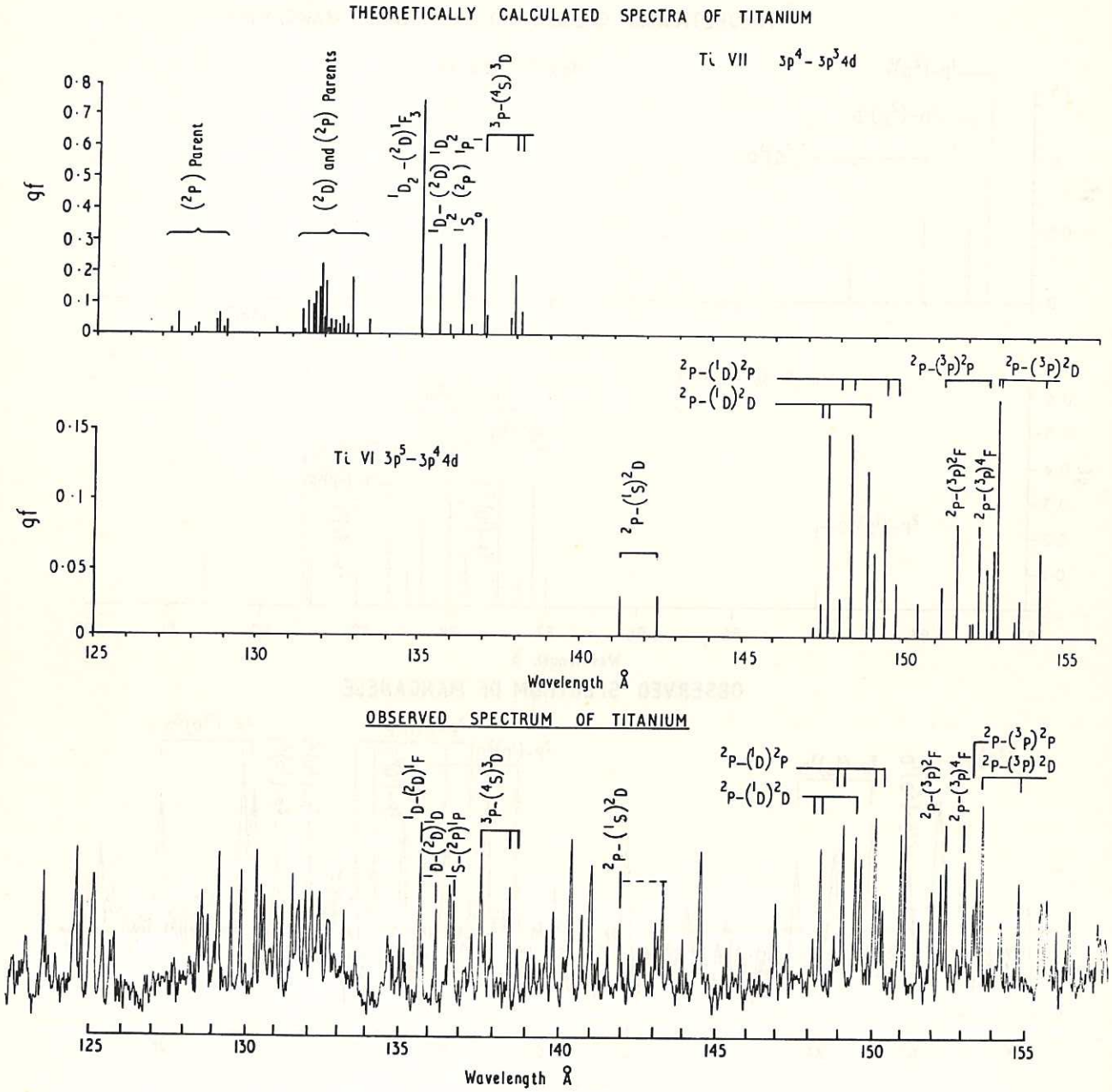

Fig. 1 (CLM-P 155)
Comparison of theoretical and experimental spectra of titanium

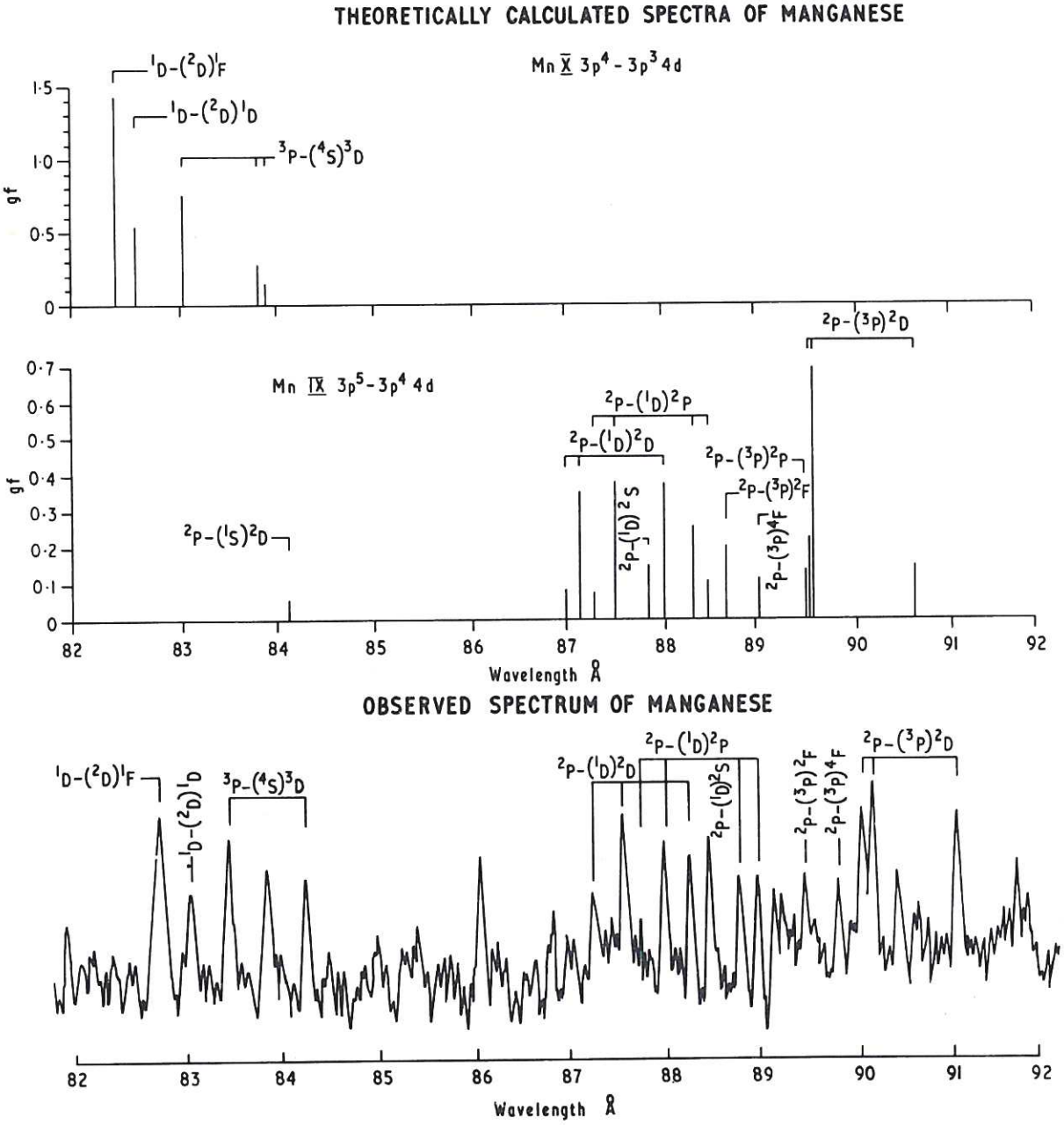

Fig. 2 (CLM-P 155)
Comparison of theoretical and experimental spectra of manganese

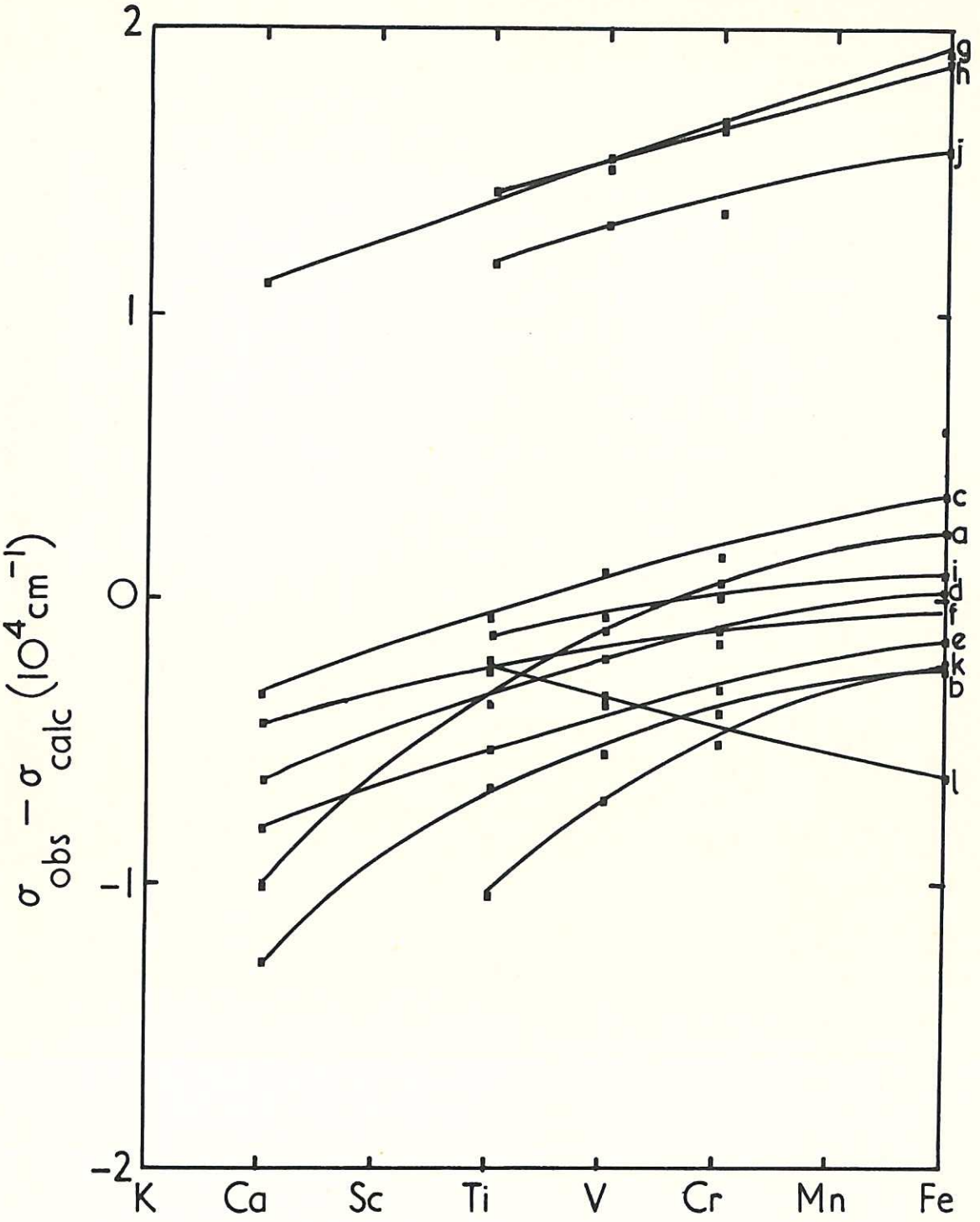

a. $3p^5\ ^2P_{1\frac{1}{2}} - 3p^4(^3P)3d'\ ^2P_{2\frac{1}{2}}$ } Fe X

b. $3p^5\ ^2P_{1\frac{1}{2}} - 3p^4(^3P)3d''\ ^2D_{2\frac{1}{2}}$ } Fe X

c. $3p^4\ ^1D_2 - 3p^3(^2D)3d''\ ^1D_2$

d. $3p^4\ ^3P_2 - 3p^3(^4S)3d''\ ^3D_3$ } Fe XI

e. $3p^4\ ^1D_2 - 3p^3(^2D)3d''\ ^1F_3$ } Fe XI

f. $3p^3\ ^2D_{2\frac{1}{2}} - 3p^2(^3P)3d'\ ^2F_{3\frac{1}{2}}$

g. $3p^3\ ^4S_{1\frac{1}{2}} - 3p^2(^3P)3d\ \ ^4P_{2\frac{1}{2}}$ } Fe XII

h. $3p^2\ ^3P_2 - 3p3d\ ^3D_3$

i. $3p^2\ ^1D_2 - 3p3d\ ^1F_3$ } Fe XIII

j. $3s^23p\ ^2P_{1\frac{1}{2}} - 3s^23d\ ^2D_{2\frac{1}{2}}$ Fe XIV

k. $3p^6\ ^1S_0 - 3p^5(^2P)3d\ ^1P_1$ Fe IX

l. $3p^5\ ^2P_{1\frac{1}{2}} - 3p^4(^3P)4d\ ^2D_{2\frac{1}{2}}$ Fe X

Fig. 3 (CLM-P155)

Differences in wave numbers between observed and computed lines due to transitions 3p-3d, 4d in Fe IX to Fe XIV, and isoelectronic ions